

# We are IntechOpen, the world's leading publisher of Open Access books Built by scientists, for scientists

6,900

Open access books available

186,000

International authors and editors

200M

Downloads

Our authors are among the

154

Countries delivered to

TOP 1%

most cited scientists

12.2%

Contributors from top 500 universities



WEB OF SCIENCE™

Selection of our books indexed in the Book Citation Index  
in Web of Science™ Core Collection (BKCI)

Interested in publishing with us?  
Contact [book.department@intechopen.com](mailto:book.department@intechopen.com)

Numbers displayed above are based on latest data collected.  
For more information visit [www.intechopen.com](http://www.intechopen.com)



# Research and Application of Solar Energy Photovoltaic-Thermal Technology

Jiang Wu and Jianxing Ren  
*School of Energy and Environmental Engineering  
Shanghai University of Electric Power  
P.R. China*

## 1. Introduction

It is believed that in the past 100 years, new technology created by mankind not only provides unprecedented power of economic development, but also provides mankind with a great ability to be harmony with the environment. Modern society should be conservation-minded society, and social life should also be energy-saving. As an inexhaustible source of new environment-friendly energy source, solar energy has become an important issue of energy research in this world.

Solar energy is a kind of renewable energy. It is rich in resources, free, non- transportation, and no pollution to the environment. Solar energy creates a new lifestyle for mankind, and takes society and human into an era of energy conservation to reduce pollution. Solar thermal conversion device industry makes solar energy technology fulfill its potential in the construction area, including hot water, heating, and air conditioning. Solar thermal conversion industry is studying solar water heating systems and building integration with the construction industry, and there have been some demonstrations. Solar air conditioning has been included in the science and technology research, and there is a large-scale demonstration plant whose economy has yet to be assessed.

As an inexhaustible security, energy-saving, environmental protection, new energy source, solar energy has attracted more and more concern in this world, and governments or companies have put their eyes on the sustainable development of the emerging solar energy field. Now, with solar technology improving continuously and the supporting of the state government, solar energy applications are increasingly widespread. Solar energy reaching the surface per second can be up to 80MW (million kilowatts), if 1% of which is transferred to electrical power, with 5% of conversion rate, then the annual generating capacity may be up to  $5.6 \times 10^{12}$  kWh, equivalent to 40 times of the current world energy consumption.

Light - heat transfer adopts sunlight to heat the water tank for potential application, which is the most common and basic form of solar thermal, and the essence of solar thermal is to collect solar radiation and convert it into heat energy by working substance. Currently, the mature technology and widely adopted solar thermal applications include solar thermal, solar water heaters, solar cookers and solar house, of which solar water heaters are the most widely used. China's solar water heater production and application began in the late 1970s, and after decades of development, China has become the largest water heater production and

consumption country in this world. Due to the factors, such as the dispersion of solar energy resources, its needing high-performance materials to get high energy transfer efficiency, and other aspects, the application of advanced solar thermal technology is not widely put into the social practice, and its research and development has a long way to go.

The main contents of this chapter include experimental research on a solar flat-plate collector, the systematic research on staged solar photovoltaic/solar thermal collectors, solar air conditioning systems and solar drying systems.

## 2. Research on solar flat-plate collector

The direct usage of solar radiation energy is to collect solar radiation using greenhouse effect to heat an object to obtain thermal energy. Currently the flat plate collector and concentrating solar collector are the two main solar energy collection devices [1, 2]. Solar collector is a key component of solar thermal system, whose manufacturing cost accounts for about half of solar water heater and its level of development processes and quality standards represent the level of development of solar thermal and solar collector technology [3].

### 2.1 Principles of solar collectors

Solar collector is a device to receive solar radiation and transfer heat to working fluid in a solar thermal system. If it adopts water as heat transfer medium, it constitutes a variety of solar water heaters, and if when using air, it yields a variety of solar dryers. Heat-absorbing board is the core of solar collector to absorb the sun's radiation to heat the heat transfer medium. Non-concentrating solar collectors apply hot-box principle, also known as the greenhouse effect, to make solar energy become inner energy [4]. Concentrating collectors use focusing principle to change directions of the sun to concentrate sunlight on a heat-absorbing body of a small area, increasing radiation intensity on unit area, so that collectors arrive at a higher temperature [5, 6]. In this chapter, a solar flat-plate collector is designed and studied.

### 2.2 Data analysis of solar flat-plate collector

The schematic diagram and picture of solar flat plate collector system are shown as Fig. 1(a) and (b). As the main parameter, temperature is measured with K-type thermocouple and TES -1310-type temperature display made in Taiwan.

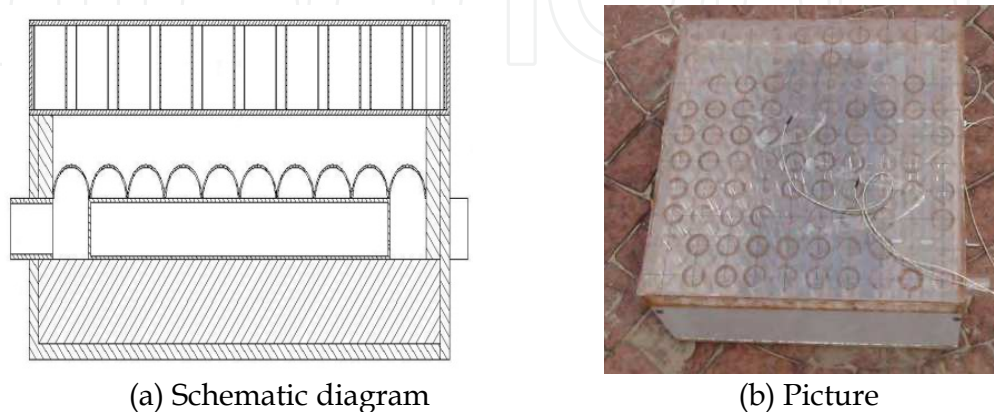


Fig. 1. Schematic diagram and picture of flat-plate solar collector

### 2.2.1 The effect of different insulation materials on the collector performance

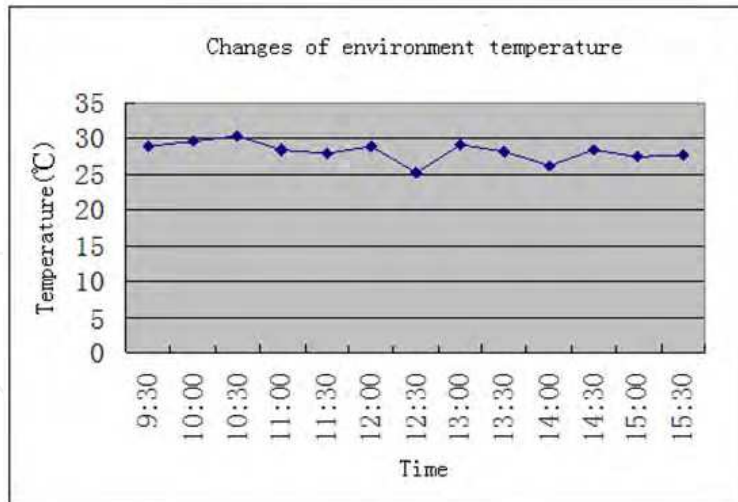
Two systems, system A and system B, are studied, and they are with 5cm thickness of glass wool and 5cm thickness of polyurethane foam board as insulation material respectively. The cover plates are both double-layer with honeycomb structure. The shell of the collector is three-ply wood, which is agglutinated by three pieces of thin wood boards. The heat-absorbing bodies are corrugated copper board, and heat transfer working medium is air. The pumping equipment is a 12V blower. When the ratio of height to width is 1.43, the effective transmittance of the cellular structure is 0.61. The comparison between different insulations is shown as Table 1.

| Time  | Atmospheric temperature (°C) | Atmospheric wind speed (m/s) | irradiation intensity | A <sub>1</sub> | A <sub>2</sub> | A <sub>3</sub> | A <sub>4</sub> | B <sub>1</sub> | B <sub>2</sub> | B <sub>3</sub> | B <sub>4</sub> |
|-------|------------------------------|------------------------------|-----------------------|----------------|----------------|----------------|----------------|----------------|----------------|----------------|----------------|
| 9:30  | 28.8                         | 0.86                         | 630.53                | 44.2           | 49.6           | 33.4           | 34.7           | 49.3           | 57.4           | 34.7           | 40.8           |
| 10:00 | 29.5                         | 0.72                         | 707.18                | 48.0           | 64.2           | 32.2           | 42.0           | 56.6           | 67.0           | 35.0           | 48.0           |
| 10:30 | 30.3                         | 1.09                         | 727.26                | 47.4           | 75.8           | 32.5           | 47.2           | 67.1           | 78.8           | 33.6           | 55.8           |
| 11:00 | 28.3                         | 1.61                         | 766.49                | 44.5           | 83.9           | 33.0           | 51.5           | 75.8           | 90.3           | 34.4           | 62.9           |
| 11:30 | 28.0                         | 1.41                         | 861.39                | 58.7           | 89.0           | 32.0           | 54.2           | 81.7           | 94.8           | 35.5           | 64.0           |
| 12:00 | 29.0                         | 0.66                         | 785.66                | 83.4           | 92.0           | 37.4           | 58.9           | 84.9           | 97.2           | 32.2           | 65.5           |
| 12:30 | 25.2                         | 0.50                         | 716.31                | 79.1           | 86.7           | 30.2           | 56.2           | 81.6           | 91.2           | 37.3           | 63.0           |
| 13:00 | 29.1                         | 1.12                         | 685.28                | 79.2           | 86.4           | 36.0           | 56.8           | 83.3           | 92.2           | 39.2           | 62.7           |
| 13:30 | 28.2                         | 1.74                         | 714.48                | 73.7           | 86.7           | 33.0           | 57.0           | 81.3           | 90.4           | 36.6           | 61.6           |
| 14:00 | 26.3                         | 0.40                         | 684.37                | 76.7           | 84.3           | 36.0           | 56.0           | 79.5           | 87.2           | 37.5           | 63.0           |
| 14:30 | 28.3                         | 0.35                         | 563.92                | 75.5           | 81.4           | 39.4           | 55.5           | 77.8           | 85.2           | 41.4           | 60.3           |
| 15:00 | 27.3                         | 0.68                         | 500.96                | 68.1           | 74.3           | 33.7           | 50.4           | 70.2           | 78.0           | 35.5           | 56.8           |
| 15:30 | 27.6                         | 0.35                         | 412.45                | 65.4           | 70.6           | 31.6           | 48.3           | 66.6           | 73.0           | 34.6           | 53.8           |

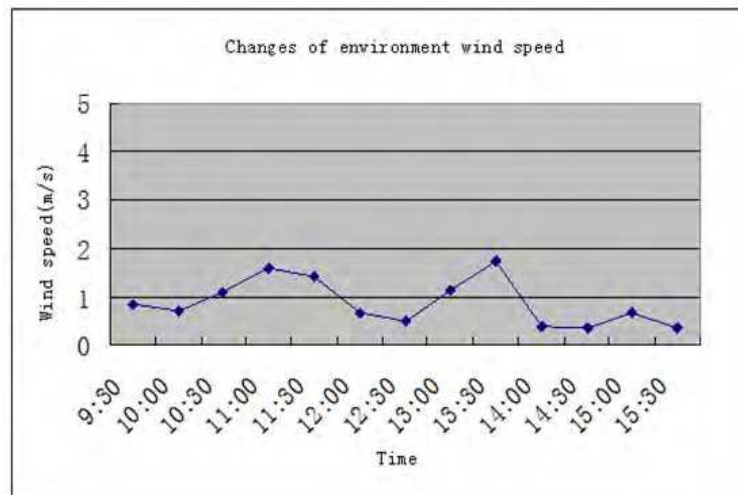
Note: The inlet velocity is 0.2 m / s; A<sub>1</sub>, A<sub>2</sub>, A<sub>3</sub>, A<sub>4</sub> are respectively the internal temperature of the cover, the surface, inlet and outlet temperature of the heat-absorbing of the system A. B<sub>1</sub>, B<sub>2</sub>, B<sub>3</sub>, B<sub>4</sub> are respectively the corresponding parameters of the system B. Different insulation material systems are used for systems A and B: A-glass wool; B-polyurethane foam board

Table 1. Comparison of experimental data between different insulation systems

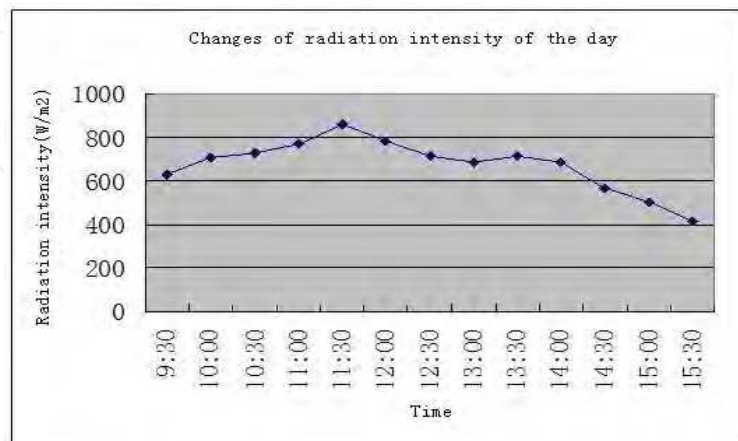
The history of the atmospheric temperature, wind speed and radiation intensity changing with time is shown as Fig. 2. Fig. 2 (a) shows that the atmospheric temperature at the daytime is relatively stable, so it has no obvious effect on the systems. From Fig. 2 (b), it can be seen that dynamic performance testing does not depend on wind speed, so the wind speed is only as the reference conditions of the atmospheric factor. Fig. 2 (c) shows that the fluctuation trend of the irradiation intensity is not unusual, so the data attained at different time are reliable.



(a) Atmospheric temperature



(b) Atmospheric wind speed



(c) Radiation intensity

Fig. 2. The history of atmospheric temperature, wind speed and radiation intensity changing with time

The history of internal temperature of the cover plate changing with time is shown in Fig. 3. It demonstrates that during the temperature-increasing process the temperature rising trend of system B is more obvious than that of system A, and system B is more stable than system A. It shows that the insulation system has effects on the plate performance during temperature rising process. The flat covers of the two systems are stable and the temperature changing trend are almost unanimously, so the effect of heat preservation system on the cover plate performance during a stable and cooling process is unobvious.

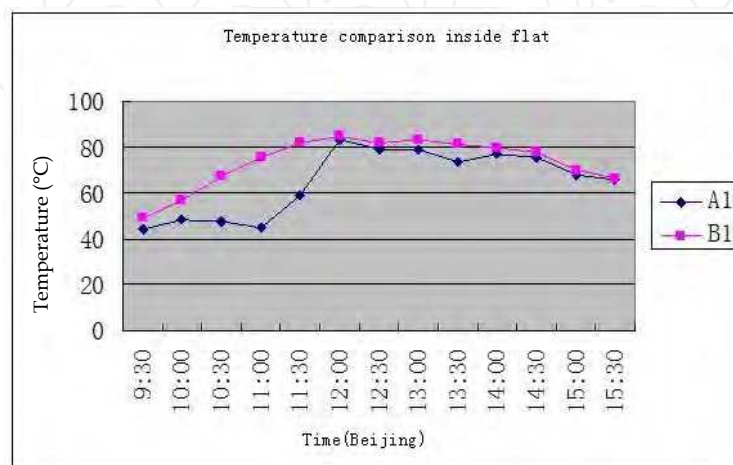


Fig. 3. The history of internal temperature of the cover plate changing with time

The history of heat absorber temperature changing with time is shown as Fig.4. The two heat-absorbing lines are almost overlapped, and the effect of heat insulation layer on heat-absorbing body is less when air, heat transfer medium, is of good flow characteristics. The effect of insulation layer on the flat cover is so small that it can be regarded because of the same cover plate structures, the working temperature of heat absorbers in the two systems may keep almost the same and not affected by the insulation structure.

The temperature at the inlet and outlet changing with irradiance is shown as Fig.5. It demonstrates that the temperature-rising speed in system B is faster than that in system A, but the irradiance is not maximum at the highest temperature. The reason is that insulation layer can delay the effect of irradiation and keep temperature-rising process in the collector continue for some time. After reaching the maximum temperature difference, system B can maintain the temperature higher than that of system A, which shows that the insulation system adopting polyurethane foam board as insulation layer is better than that of glass wool insulation during the heating process till the highest temperature. But it should be noted that the temperature transition in system A with the glass wool insulation layer is more stable at a relatively low temperature and irradiance condition, while system B is with a sudden drop point, which illustrates that glass wool insulation has better insulation performance when heat released by the working substance is in the end. As the economic advantage of glass wool is far greater than that of polyurethane foam, to achieve the best insulation, polyurethane foam may be considered as insulation material used at the zone closer to the working fluid, and glass wool is used as insulation at the external wall where temperature is relatively low, so as to reduce the cost of the system.

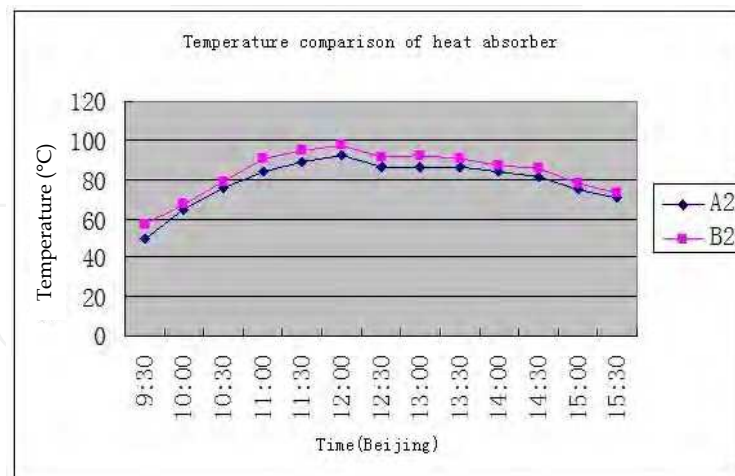


Fig. 4. The history of the heat absorber temperature changing with time

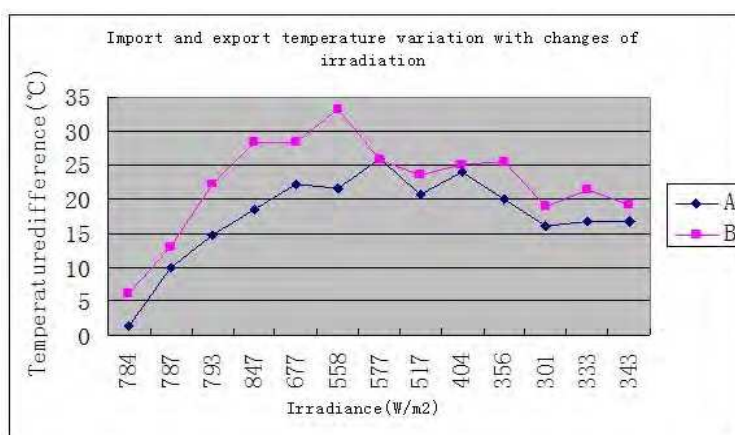


Fig. 5. The inlet and outlet temperature changing with the irradiance

### 2.2.2 The comparative experiments and data analysis on the cover performance

In this set of experiments, single-layer PC board and double-layer honeycomb structure are applied as the covers for system A and B, respectively. In the two systems, the shells are both wooden three plywood, the insulation are both polyurethane foam, and heat-absorbing bodies are both waveform copper plates. Temperature measurement points are on the surfaces of the cover (two points) and heat-absorbing surface (two points) respectively.

The history of heat-absorbing body temperature of system A, B changing with time is shown as Fig. 7. It demonstrates that ignoring other factors, although due to the difference placement or angle, the initial temperature of system A is higher than that of system B, the heating rate of system B is significantly higher than that of system A. It shows that there are heat losses in the two systems during the endothermic process, but the heat loss of system B is significantly less than that of system A when other conditions are the same. It tells that honeycomb structure plate plays a great role on inhibition of the heat loss due to air convection inside the cover.

| Time  | Atmospheric temperature (°C) | Atmospheric wind speed (m/s) | Irradiance ( $w/ m^2$ ) | A <sub>1</sub> | A <sub>2</sub> | A <sub>3</sub> | A <sub>4</sub> | B <sub>1</sub> | B <sub>2</sub> | B <sub>3</sub> | B <sub>4</sub> |
|-------|------------------------------|------------------------------|-------------------------|----------------|----------------|----------------|----------------|----------------|----------------|----------------|----------------|
| 9:30  | 27.2                         | 0.55                         | 783.83                  | 41.6           | 38.5           | 69.1           | 69.7           | 37.5           | 35.7           | 54.4           | 55.7           |
| 10:00 | 29.2                         | 1.57                         | 787.48                  | 48.2           | 46.1           | 82.0           | 81.1           | 43.1           | 42.0           | 70.7           | 68.9           |
| 10:30 | 29.9                         | 0.99                         | 792.96                  | 49.5           | 48.5           | 82.6           | 80.7           | 43.0           | 42.3           | 72.8           | 70.3           |
| 11:00 | 27.3                         | 1.33                         | 846.79                  | 49.6           | 42.0           | 85.0           | 86.5           | 41.3           | 42.8           | 78.2           | 76.1           |
| 11:30 | 25.6                         | 0.57                         | 677.07                  | 49.4           | 45.0           | 86.1           | 88.3           | 45.3           | 47.0           | 85.2           | 83.9           |
| 12:00 | 27.6                         | 0.73                         | 558.46                  | 47.2           | 43.4           | 83.2           | 86.6           | 46.1           | 46.5           | 86.0           | 85.1           |
| 12:30 | 26.3                         | 0.41                         | 576.70                  | 44.7           | 43.3           | 77.9           | 77.5           | 46.3           | 48.3           | 85.4           | 84.2           |
| 13:00 | 28.3                         | 1.72                         | 517.38                  | 45.9           | 41.2           | 82.2           | 80.7           | 44.7           | 45.7           | 83.4           | 82.3           |
| 13:30 | 29.3                         | 0.33                         | 404.23                  | 41.8           | 38.0           | 71.9           | 71.4           | 40.2           | 39.9           | 78.3           | 78.5           |
| 14:00 | 27.5                         | 2.42                         | 355.87                  | 38.3           | 35.2           | 61.3           | 60.9           | 36.5           | 37.5           | 67.7           | 66.6           |
| 14:30 | 25.9                         | 0.48                         | 301.12                  | 38.6           | 36.1           | 58.9           | 59.6           | 38.6           | 38.5           | 65.4           | 64.0           |
| 15:00 | 25.2                         | 2.58                         | 333.06                  | 43.6           | 39.5           | 70.5           | 68.2           | 40.2           | 40.3           | 68.1           | 67.3           |
| 15:30 | 26.5                         | 1.63                         | 343.10                  | 39.0           | 35.9           | 61.6           | 60.4           | 37.2           | 36.5           | 64.3           | 63.7           |

Note: A<sub>1</sub> and A<sub>2</sub> are the temperature on the cover surface of system A at the different sites, A<sub>3</sub> and A<sub>4</sub> are the temperature on the heat-absorbing surface of system A at different sites, taking the average as the calculation value. B<sub>1</sub>, B<sub>2</sub>, B<sub>3</sub> and B<sub>4</sub> are the corresponding parameters of system B.

Table 2. Comparison between experimental data of the cover performance



Fig. 6. Comparative testing on cover performance

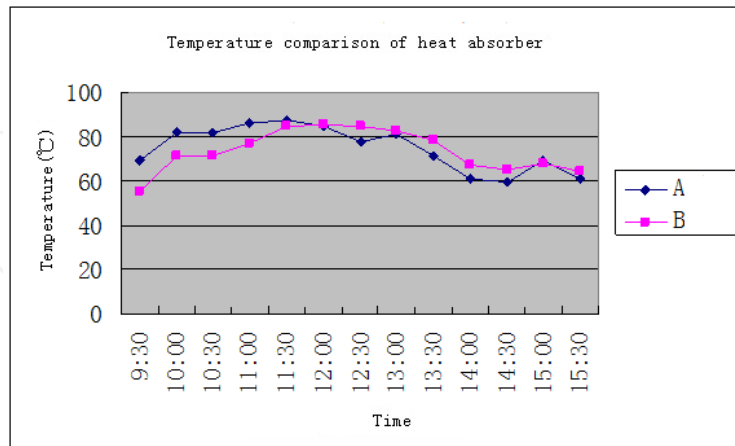
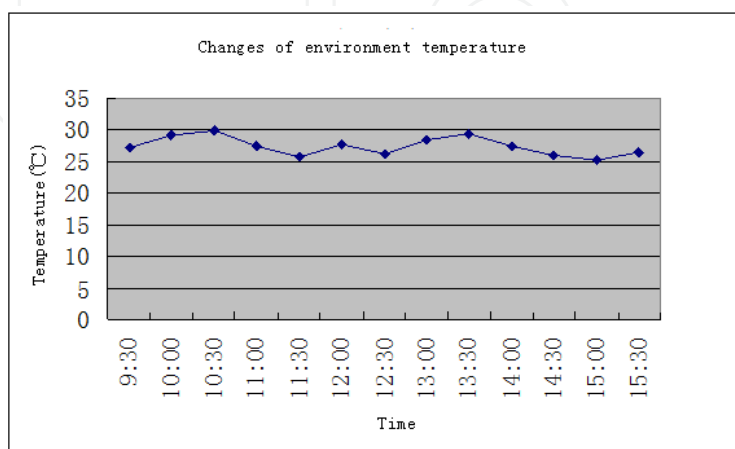
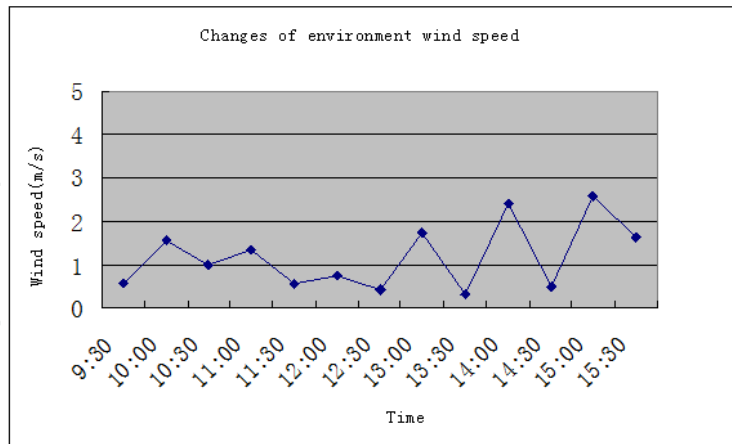


Fig. 7. Heat-absorbing body temperature changing history

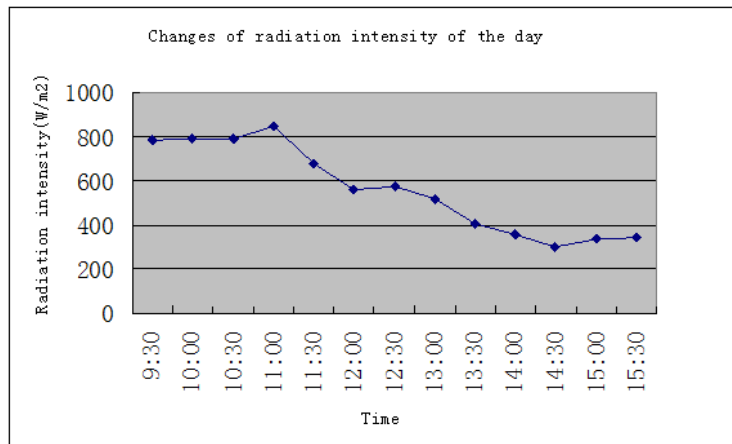
In the comparative experiments on the cover performance, the changing of atmospheric temperature, wind speed, radiation intensity, and cover surface temperature with time is shown as Fig. 8 (a) to (d). From Fig. 8 (a) and (b), it can be seen that the changing of atmospheric temperature is stable, and its fluctuation is less than 5 °C. Fluctuation of wind speed is also small, less than 2m/s. From Fig. 8 (c), it can be seen that radiant intensity reaches the maximum at 11 a.m., and then as the time goes on, the radiation intensity declines gradually. According to table 2, the experimental conditions meet the requirements of dynamic performance testing. From Fig. 8 (d), it can be seen that the atmospheric temperatures are the same, and the covers are both PC board material, so that the surface temperature difference is very little, and the changing trends are the same. Therefore, the cover structure will not affect solar energy absorption of the cover surface.



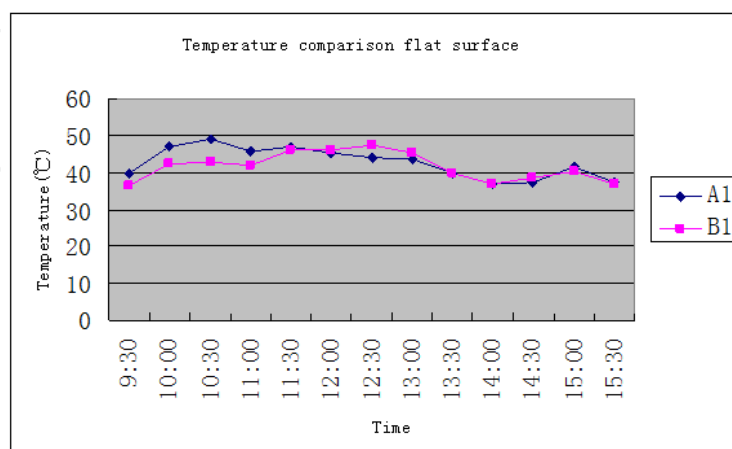
(a) Atmospheric temperature



(b) Atmospheric wind speed



(c) Radiation intensity



(d) Cover surface temperature

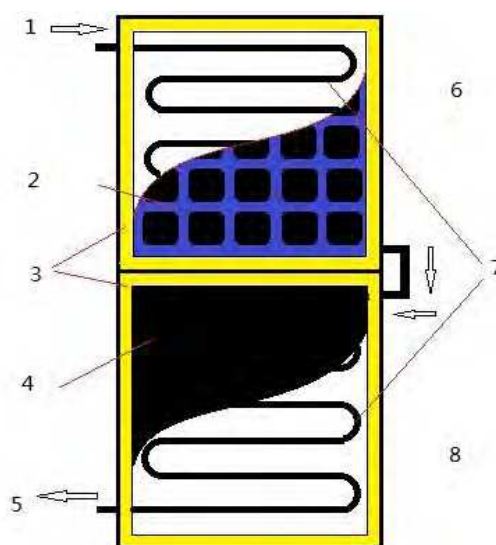
Fig. 8. The history of some parameters changing with time

### 3. Staged solar photovoltaic / thermal collector

Solar cell is the core unit of solar photovoltaic power generation. Currently the commercial solar cells are mainly silicon solar cells, including mono-crystalline, polycrystalline and amorphous silicon solar cells. The effects of temperature on silicon solar cells mainly include open circuit voltage, short circuit current, peak power and other parameters of the solar cells [7-10]. In the photovoltaic solar thermal flat-plate collector PV/T, there is a conflict between the photovoltaic power generation efficiency and solar thermal heat production efficiency, which means that one of them decreases while the other increases. How to further lower temperature of the solar cell plate and optimize the whole PV/T system to improve photovoltaic power generation efficiency of the PV/T collectors is the main study content of our research, which has important significance to improve the integrated utilization of PV/T solar collectors.

#### 3.1 Structure and working principle of PV / thermal collector

The main structure of the PV/thermal collector consists of cover, solar modules, heat-absorbing plate, gas or liquid flow path, the edge, back insulation, metal frame and so on, which is without big difference from the traditional photovoltaic solar thermal (PV/T) collector system, and it is shown as Fig. 9. However the system adopts a staged PV/T system, which is different from the traditional photovoltaic solar thermal (PV/T) collector system. The absorber plate of this solar panel collector is no longer composite as a whole, which applies staged form, i.e., it is divided into two parts: the primary stage is solar photovoltaic system and the secondary stage is solar thermal system. There is no direct heat exchange in the space between the two parts, and heat transfer is through the cooling pipes connected between them.



1. Water inlet 2. Solar panels 3. Insulation layer 4. Absorber plate 5. Water outlet  
6. The primary stage system 7. Cooling water channels 8. The secondary stage system

Fig. 9. System diagram of staged type PV/T

For the primary stage of the solar cell system, usually the photoelectric conversion efficiency is 15% to 17% by using single crystal silicon solar panels, and the rest of the solar radiation

will transform into heat, while the efficiency of solar panels will decrease with the temperature rising on the board surface, which will make solar panels enter a vicious cycle. For the secondary stage of solar thermal system, the solar radiation heat is mainly absorbed by the heat-absorbing panels, and then the heat is delivered to the cooling substance so as to heat the working fluid. The heat production efficiency and the quality of output water of the system will be improved when the temperature at the inlet of the working fluid increases.

The heat on the solar plate board surface is taken away by cooling water flowing through the primary stage, which can increase the power generation efficiency of the solar photovoltaic. The heat of solar collectors is absorbed through the secondary stage by the cooling water, whose temperature is increased by first stage. The flat-plate solar collector efficiency increases because of the temperature rising of inlet working fluid, which in turn makes the overall utilization efficiency of solar energy increase.

### **3.2 Overall structural design and layout of solar photovoltaic / thermal collector**

#### **3.2.1 The size of solar photovoltaic / thermal collector**

The design concept of staged photovoltaic solar thermal collector is proposed in this chapter, and the collector consists of two parts. The primary part is the ordinary solar photovoltaic thermal collector mainly for power generation, however in this design, water is adopted as the working fluid for the thermal collector to cool the panels so as to improve its efficiency and the water is preliminarily heated. The secondary part is a flat-plate collector, playing the role of thermal collector, which is used to heat water flowing out of the primary part.

The structure of the staged collector is shown as Fig. 9. The upper is the primary part covered with solar panels, and the lower side is the secondary part, whose bottom is covered with blackened copper to enhance heat absorption.

The equipment specifications are as followings:

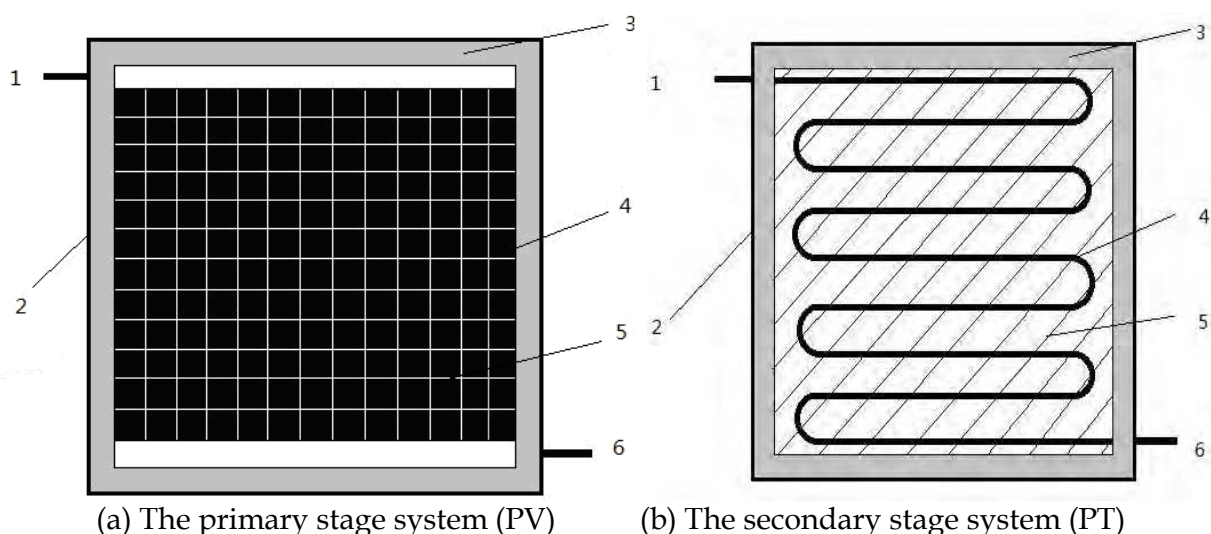
1. Cabinet: Its material adopts galvanized iron sheet with dimension  $1000 \times 500 \times 150$ mm.
2. Endothermic board: Endothermic board adopts 1mm thickness of copper with the surface sprayed black in order to reduce glare and enhance the endothermic effect.
3. The circulation line: The circulation line applies copper pipe, whose diameter is 10mm, to enhance the heat-absorbing and heat transfer, and the copper surface is blackened with black paint and fixed on the back of absorber plate closely.
4. Transparent cover: It uses ordinary glass, and its size is  $505 \times 490 \times 4$ mm.
5. Insulation: Insulation adopts fiberglass, whose thickness is about 50mm.
6. Solar panels: Its power is 20W, and its voltage is 17.6V, current is 1.14A, open circuit voltage is 21.6V, short circuit current is 1.33A, and its size is  $426 \times 406 \times 30$ mm, weight 2.6kg.

#### **3.2.2 The distribution of PV/T heat collector**

In this issue, the distribution of PV/T heat collector is two-stage, i.e., the primary stage is photovoltaic subsystem and the secondary stage is photo-thermal subsystem. The principle of this system has been discussed above. Now we focus on its dimensions.

The primary-stage system (PV system) is shown as Fig. 10(a). The dimensions of the system is 500×500×150 mm, and its bottom and all-around are covered with the heat insulating material with 50mm of thickness. Its inner space is with the dimensions of 400×400mm, where a single crystal silicon solar panel of 400×300mm is arranged in it. S-shaped cooling line made of copper, whose outer diameter is 10mm, is installed on the back of solar panel. The copper tube is closely fixed on the back of solar panel to fully absorb the heat and to decrease the temperature of the latter, and heat cooling water inside the tube at the same time. There is an inlet and an outlet of water in the primary stage system.

The secondary stage system (PT system) is shown as Fig. 10(b). The overall size is equal to the primary stage system. The size of heat-absorbing aluminum plate is 400×400mm, which is mounted inside the system. It is covered with black heat-absorbing paint. Compared with previous arrangement, the S-shaped copper tube is arranged on heat-absorbing aluminum plate. It closely contacts the heat-absorbing plate through fiche to enhance its heat transfer efficiency. Furthermore, the copper tube is covered with black heat-absorbing paint to absorb radiation directly. In the secondary stage system, there exists an inlet and an outlet of water as well.



1. Inlet 2. External wall 3. Heat insulating material 4. S-shaped tube 5. Heat-absorbing plane 6. Outlet  
Fig. 10. The primary and secondary stages of the PV/T system

### 3.3 The experimental system of PV/T heat collector

#### 3.3.1 The system transform valve

A valve, which is called transform valve, is used to link the primary and the secondary stage systems to control the connection or disconnection of the two stage systems to conduct a single PV, single PT and PV/T experiment studied in this chapter. The overall system scheme is shown as Fig. 13. When transform valve is closed and the auxiliary valve is open, the primary stage system is dependent from the secondary stage, and the experiment can be conducted on the primary and secondary stage respectively. When the transform valve is open and the auxiliary valve is closed, the primary is linked to the secondary stage system, and the cooling water or air enters into the primary stage system through the inlet and take

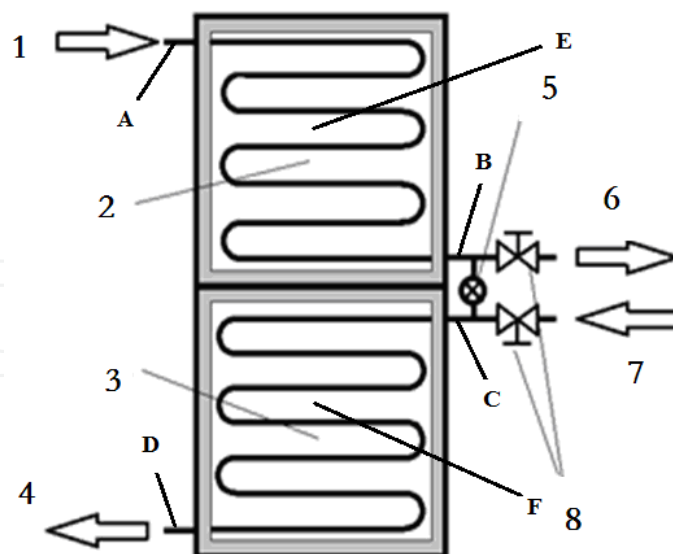
the heat of solar panel away. Then, it continues to absorb heat when it enters into the secondary stage system, which produces hot water and hot air.

### 3.3.2 The distribution of data collection points

In order to measure the data better, high accuracy thermocouple is mounted on each monitor node shown as Fig.11. Thermocouples A, B, C and D are to measure the inlet and outlet temperature of the primary and secondary stage system, respectively. Thermocouple E and F are to measure internal cavity temperature of the primary and secondary stage system respectively. At the same time, there are testing points to measure the atmospheric temperature, wind speed, voltage and current of the solar panel.

### 3.3.3 The principle of measurement

The electric performance testing of the solar panel may be attributed to test its voltage current characteristics. Since the voltage current characteristics is relative to the testing conditions, the performance of solar panel needs to be tested under standard condition or the measured results need to be transformed into standard condition. The standard testing condition consists of standard sunshine, which includes standard spectrum and radiation, and standard testing temperature, which can be controlled manually. The standard sunshine can be simulated or attained in nature. When simulated sunshine is applied, the spectrum depends on the sort of electric light source and filtering and reflecting systems. Radiation can be adjusted through the calibrated value of the short-circuit current of the solar battery. In order to reduce unmatched error of the spectrum, the spectrum of simulated sunshine should be close to the standard sunshine spectrum or the standard solar battery, whose response is almost the same as that of the tested battery, should be chosen<sup>[11,12]</sup>.



1. The primary stage outlet system 2. The primary stage system 3. The secondary stage system 4. The secondary stage outlet system 5. Transform valve 6. The primary stage outlet 7. The secondary stage inlet system 8. Auxiliary valve A. Thermocouple A B. Thermocouple B C. Thermocouple C D. Thermocouple D E. Thermocouple E F. Thermocouple F

Fig. 11. The valve control and distribution of data acquisition diagram

### 3.3.4 Electric performance testing conditions

#### a) The standard testing conditions

Overall radiation is measured by AM 1.5 standard action spectrum. The radiation is  $1000\text{W}/\text{m}^2$ , and the testing temperature is  $25^\circ\text{C}$ .

As for the standard testing, the tolerance error of standard temperature measurement is  $\pm 1^\circ\text{C}$ , while the tolerance error is  $\pm 2^\circ\text{C}$  for the nonstandard testing. If the testing can only be conducted under nonstandard condition due to the restriction of the objective condition, the tested results should be transformed into the standard testing condition.

#### b) Testing devices and apparatus

The testing devices and apparatus include standard solar battery, voltmeter, ammeter, sample resistance, load resistance, thermometer, and indoor tested light source. The standard solar battery is used to adjust the radiation of tested light source. When AM 1.5 standard solar battery is tested, the radiation is adjusted by secondary-rank AM 1.5 standard. In nonstandard measurement, the radiation is only adjusted by AM 1.5 standard. The accuracy of voltmeter is no less than class 0.5 and its internal resistance is no less than  $20\text{k}\Omega/\text{V}$ , generally using digital voltmeter. The accuracy of ammeter is no less than class 0.5 and its internal resistance should guarantee the tested voltage is no more than 3% of open circuit voltage when short circuit current is tested. When better accuracy is necessary, it can take advantage of voltage's linear relationship with current to deduce short circuit current when full short circuit is below 3% of open circuit voltage. The current can be measured by measuring the voltage drop of sample resistance through digital millivolt meter.

The product of short circuit current and sample resistance is no more than 3% of open circuit voltage. Load resistance can be adjusted from 0 to more than  $10\text{k}\Omega$  smoothly. Subsequent power volume should be guaranteed to the accuracy, which is influenced by heating power produced by electricity. When the variable resistance can't meet condition above, an equal electron variable load should be adopted. The error of thermometer or thermometric coefficient is no more than  $\pm 0.5^\circ\text{C}$ . Response time of the testing system is no more than 1s. The radiation, uneven extent of radiation, stability, accuracy, and spectral distribution must meet some demand.

#### c) Testing items

The testing items include open circuit current ( $V_{oc}$ ), short circuit current ( $I_{sc}$ ), optimum operating voltage ( $V_m$ ), optimum operating current ( $I_m$ ), maximum output ( $P_m$ ), photoelectric conversion efficiency ( $\eta$ ), filling factor (FF), I–V characteristic curve, short circuit current temperature coefficient ( $\alpha$ ), open circuit voltage temperature coefficient ( $\beta$ ), internal series connection resistance (R), internal parallel connection resistance ( $R_{sh}$ ).

#### d) Basic testing method

Of the above testing items, open circuit voltage and short circuit current are tested by ammeter directly, and the other parameters are calculated through voltage current characteristics. The voltage current characteristics of solar battery is tested under standard sunshine, solar simulator or other equal solar simulators.

### e) Convert nonstandard testing condition into standard testing condition

When the testing temperature and radiation differs from the standard condition, it can be corrected according to the following equations:

$$I_2 = I_1 + I_{sc} \left( \frac{I_{SR}}{I_{MR}} - 1 \right) + \alpha (T_2 - T_1) \quad (1)$$

$$V_2 = V_1 - R_s (I_2 - I_1) - k I_2 (T_2 - T_1) + \beta (T_2 - T_1) \quad (2)$$

Where  $I_1$ ,  $V_1$ : Tested voltage, tested current or the parameter to be corrected;  $I_2$ ,  $V_2$ : Corrected result;  $I_{sc}$ : Short circuit current;  $I_{MR}$ : Short circuit current of standard battery under practical condition;  $T_1$ : Testing temperature;  $T_2$ : Standard testing temperature;  $R_s$ : The internal series electric resistance of tested battery;  $k$ : Curve correction factor, which can be set as  $1.25 \times 10^{-3} \Omega/^\circ\text{C}$ ;  $\alpha$ : Short circuit current temperature coefficient under standard radiation condition and certain temperature window;  $\beta$ : Open circuit voltage temperature coefficient under standard radiation condition and certain temperature window.

## 3.4 Experimental data analysis

### 3.4.1 Experimental apparatus

The apparatus needed in the experiment for solar panel PV/T heat collector consists of distributed solar panel PV collector, TRM-PD artificial solar panel simulator, 10mm outer diameter of rubber tube, 18W pump, 12VDC electrical source, K thermocouple, data acquisition card, Agilent 34970A data acquisition and a computer.

### 3.4.2 Data analysis

The experimental data are collected and recorded by data acquisition system, and exported to CSV format or excel charts. Different variation curve corresponding temperature, current, and the voltage are as follows.

The relationship between current and voltage, and the history of voltage and current changing with the surface temperature are shown as Fig. 12 and Fig. 13 (a) and (b) respectively. It can be seen from Fig. 12 that the current curve and voltage curve merged gradually with the changing of time, and they combined at last. The current and voltage affected each other, and the current has the same trend as the voltage, i.e., when voltage goes up or down, the current also goes up and down. As shown in Fig. 12, the current curve is steady, so that no matter how the flux of cooling water varies, the voltage curve is almost without any effect. The current drops down immediately at the data point of 333, and after this point, the current is around 0.12A. There are some abnormal points in Fig. 12, which are assumed due to the random error [11, 13].

As shown in Fig. 13 (a) and (b), the higher the surface temperature, the lower the output voltage. However, the curve is relatively gentle. It is obvious that the higher the surface temperature the lower the output current. There are some abnormal points due to error. And then, it can be seen that the generating efficiency of solar panel is greatly influenced by surface temperature of solar panel. Furthermore, the higher the surface temperature it has,

the lower the generating efficiency. It agrees well with the initial hypothesis of the experiment. Through data analysis, the stable data can be chosen from each flux part. The average data at each flux are shown as table 3.

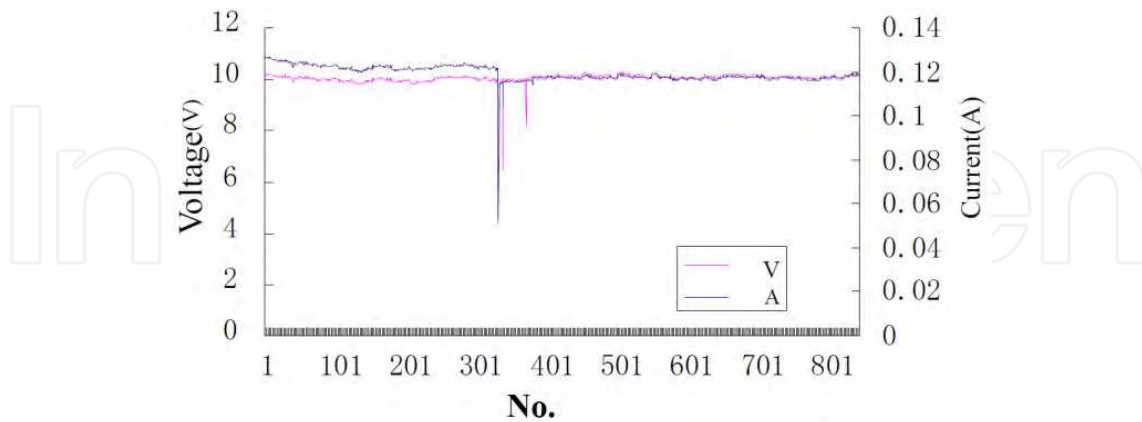


Fig. 12. Relationship between current and voltage

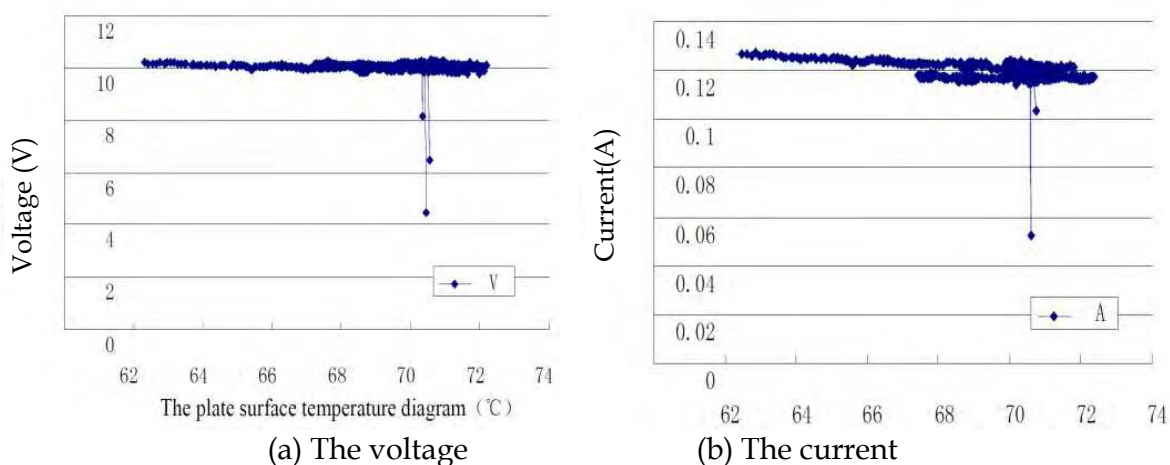


Fig. 13. The history of voltage and current changing with surface temperature

Due to the limited range of the data acquisition instrument, the streaming triage method is used to collect the data. An electric resistance with the same resistance value as that of the data acquisition instrument is paralleled into the data collection section to share the electric current. The diagram is shown as Fig. 14.

It can be attained from Fig. 14:

$$U_i = U_r = U_{total} \tag{3}$$

$$I_{total} = I_i + I_r = I_i + U_{total} / R \tag{4}$$

Where  $U_{total}$  is the voltage of the cell plate,  $U_i$  and  $U_r$  are the voltage of collector and the voltage between the two ends of the parallel resistance respectively;  $I_{total}$  is the current of the panels;  $I_i$  and  $I_r$  are the current flowing through the collector and the parallel resistance;  $R$  is the parallel resistance,  $10\Omega$ .

Therefore, generating power of the solar panels is calculated as follows:

$$P_{total} = P_i + P_r = U_i \cdot I_i + \frac{U^2}{R} \tag{5}$$

Based on the data in table 3, according to eq. (5), it can get  $P_{total}$  and  $P_{average}$  shown in table 4.

|   |        |        |        |        |        |        |
|---|--------|--------|--------|--------|--------|--------|
| Flux (L/h)                                    | 2.647  | 3.103  | 7.895  | 15.000 | 27.692 | 36.000 |
| Inlet temperature (°C)                        | 28.809 | 29.155 | 27.808 | 28.012 | 28.088 | 28.049 |
| Outlet temperature of the primary stage (°C)  | 39.206 | 42.445 | 34.967 | 32.021 | 31.905 | 30.026 |
| Outlet temperature (°C)                       | 45.718 | 50.780 | 38.633 | 34.551 | 34.271 | 31.356 |
| Heat-absorbing plate Temperature (°C)         | 52.507 | 64.114 | 51.873 | 50.649 | 52.356 | 50.082 |
| Glass Cover-Plate Temperature (°C)            | 63.945 | 66.650 | 68.197 | 55.286 | 68.084 | 66.934 |
| Back surface Temperature of solar Panel (°C)  | 67.014 | 69.870 | 70.851 | 72.231 | 72.604 | 71.927 |
| Front surface Temperature of solar Panel (°C) | 67.262 | 69.591 | 71.242 | 72.582 | 73.084 | 72.128 |
| Atmospheric temperature (°C)                  | 29.581 | 30.258 | 29.770 | 30.506 | 30.169 | 30.409 |
| Voltage (V)                                   | 10.083 | 10.088 | 9.940  | 9.962  | 10.152 | 10.176 |
| Current (A)                                   | 0.1246 | 0.1170 | 0.1216 | 0.1201 | 0.1176 | 0.1167 |

Table 3. Average Tested Data

|                   |        |        |        |        |        |        |
|-------------------|--------|--------|--------|--------|--------|--------|
| $Q_v$ (L/h)       | 2.647  | 3.103  | 7.895  | 15.000 | 27.692 | 36.000 |
| $P_{total}$ (W)   | 11.423 | 11.357 | 11.089 | 11.117 | 11.500 | 11.543 |
| $P_{average}$ (W) | 11.34  |        |        |        |        |        |

Table 4. The  $P_{total}$  and  $P_{average}$  at different  $Q_v$

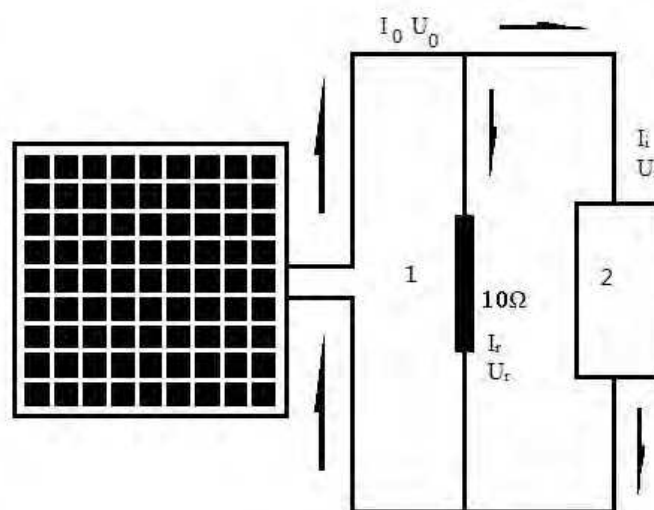


Fig. 14. The diagram of data acquisition circuit

The light intensity of solar simulator that the system adopts is 800W and the effective area used in the system is  $400 \times 300 \text{ mm}^2$ . Therefore, the input power of the solar panels can be calculated as following.

$$P_{inlet} = 800W / m^2 \times 0.12m^2 = 96W \quad (6)$$

The utilization efficiency of solar system can be calculated as following:

$$\eta = \frac{P_{average}}{P_{inlet}} \times 100\% = 11.8\% \quad (7)$$

The generation powers corresponding to the above flux are shown as Fig. 15.

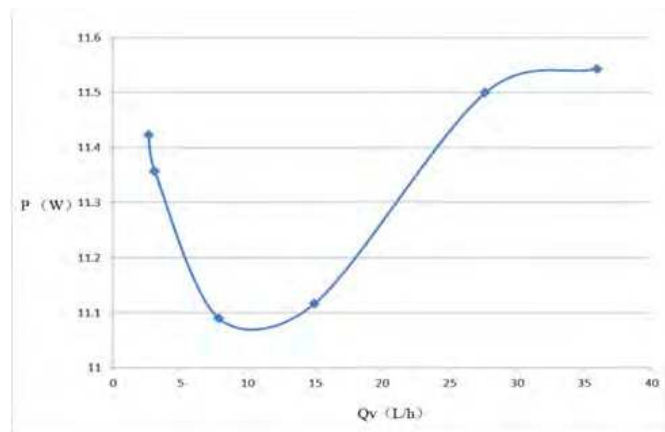


Fig. 15. The generation power changing with the flux

It can be seen from Fig. 15 that generating power of the solar panels decreased and then increased with the increasing of the cooling water flow. This may be because the board surface temperature is not high when the panels start to work, and the battery plate board surface is of higher photoelectric conversion efficiency. But with the increasing of the working hours, accumulation of heat on the plate is increasing more and more, and at the same time the cooling water flowing on the back surface of the solar panels is so small that it can't transfer heat of the battery plate board's surface out well, which makes solar panels generating power present a downward trend at this stage. When the cooling water flow rate on the back surface of the panels increased to 10L/h or so, the generation power of panels began to increase with the increasing flow rate of cooling water and when the flow rate reached up to 30L/h or so, the curve of the generation power of the panels becomes stable. This shows that when flow rate of the cooling water is between 10L/h and 30L/h, the effect of cooling panels is better, which makes the temperature of battery plate board surface be controlled, so that the generating power of the solar panels gradually increased. When flow rate of the cooling water is higher than 30L/h, the generation power of the solar panel hardly changes with the flow rate, and it can be inferred that 30L/h is the best flow rate for the cooling water.

In the experiment, power output of the solar panel is 20W, radiation intensity of the solar simulator is 800W, and the rated power output of the solar panel is calibrated with the solar radiation output at 1000W. The output power of the solar panel is basically linear with photovoltaic intensity, so the power output under 800W of radiation intensity is

$$P_{800} = 20W \times 800W / 1000W = 16W \quad (8)$$

$P_{\text{average}}$ , the calculated average power output of the generation system, equals to 11.34 W, which is 4.66W less than the output power when radiation intensity is at 800W, that is to say, the actual power output of the generation system is 70.88% of the rated power output.

#### 4. Solar air-conditioning/heating system

At present, the solar energy air-conditioning becomes the key research and development of the energy projects in some countries [14, 15]. In the late 1970s, with the development of solar energy technology, solar air conditioning technology emerged. The research on using solar energy to provide heating and cooling for the buildings has been developed rapidly in many ways. New industrial district of solar energy has been born in many countries and many solar energy devices have been commercialized. International and regional academic, exhibition and cooperation have become frequently and many countries allocated money to subsidize solar energy utilization every year. However solar air-conditioning industry is still in the developing stage [16, 17], and the market still needs time to be mature.

The solar energy air conditioning is developed well mainly in Italy, Spain, Germany, the United States, Japan, Korea, Singapore, and Hong Kong [18]. China mainland has conducted a lot of research on the usage of solar heating and cooling. The first small-scale solar energy building was built in Gansu, China in 1977, mainly for heating. And a practical large-scale solar water heating and air conditioning system was built in Jiangmen, by Guangzhou Institute of Energy in 1998, but the use of solar energy cooling in summer and heating in winter and providing hot water for living in the transition seasons is still in its initial stage. Furthermore, with improvement of living standard and formation of high income class, the demand on the indoor and outdoor environment of constructions is gradually increasing, so that the combination of solar and villa construction have a bright prospect of development because of its non-pollution characteristics [19].

In summer, the hot water heated by heat collector goes to the storage tank. When the water temperature reaches a certain value, the storage tank provides water, the heat medium, to the refrigeration machine. When hot water comes out of the refrigeration machine, its temperature drops and as the heat medium, it goes back to the storage tank to be heated by the solar collector. Refrigerating machine produces chilled water for air conditioning box to achieve the purpose of air conditioning. When solar radiation is insufficient to provide enough heat for high temperature hot medium water, the auxiliary heat source is turned on. In winter, hot water heated by solar collector goes to storage tank, and when its temperature reaches a certain value, the heat storage water tank directly provides hot water to air conditioner box. When heat provided by solar radiation is not sufficient, the auxiliary heat source will switch on. During the transition season, the hot water heated by the collector flows through the heat exchanger into the hot water tank, to heat water in it.

##### 4.1 The purpose of the research on solar air conditioning / heating system

With the improvement of living standard, human demand for energy is increasing day by day. But along with the price of the coal and demand of air pollution emission controls gradually increase, the cost of electricity has arisen. So the development of efficient, environmentally friendly and safe energy has great prospects.

At present, there are two main ways to use solar energy, i.e., photovoltaic and solar thermal. PV is no good chance to develop due to its high costs. Photo-thermal is fairly popular in people's living by using solar water heater [13]. However solar water heater only plays a small part for living energy supply. Furthermore, currently the solar cells of single crystal and polycrystalline silicon on the market have an average efficiency of around 15%.

The design of the solar air conditioning /heating system in this chapter occupies little electricity, using clean energy to cool in the summer and heat in the winter. It makes full use of light energy, through photovoltaic and photo thermal effects to produce heat and power generation at the same time. The gravity heat pipe is installed on the back surface of a solar panel, so that heat from the solar panel can be transferred to the house. Thus, the photovoltaic efficiency of the solar cell is obviously improved without changing its solar board structure.

Traditional heating and heat preservation facilities are adopted for the solar panels and solar collector individually. But solar energy density is so low that considerable area of the collection and conversion equipment are often required to get some conversion power, whose cost is very high. In fact, how to make good use of solar energy for building energy saving, and some passive solar application facilities, which combine heating in winter with heat insulation in summer, are even now continuing to be studied [20].

Currently, many organizations have developed the system similar to solar air-conditioning system, but the actual mature technology of solar air conditioning is still very rare [21].

A solar air conditioning/heating system has been developed in this chapter, and the efficiency of photovoltaic solar panel system increases 6% and output power of the simulated system in the experiment is 558.66w. In heat supply conditions in winter, the heat exchanger can output 467w heat to the house. It can accomplish the combination of heating in winter and cooling in summer, and it can save energy and improve the efficiency of photovoltaic solar panels on the market. Based on the photovoltaic and photoelectric effects, the system applies solar radiation as the energy source so that it can reduce energy consumption and become a heating-cooling two-way solar air conditioning / heating system.

## **4.2 Experimental study on solar air conditioning / heating system**

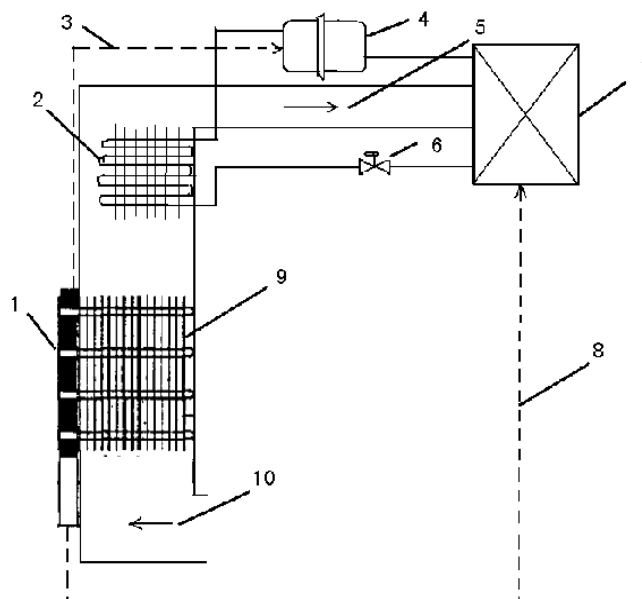
### **4.2.1 Description of the solar air conditioning / heating system**

The solar air conditioning / heating system in this chapter is as the following:

1. The solar air conditioning / heating system in this chapter has the function of cooling in the summer and heating in the winter using clean energy, with a little or without electricity.
2. The system makes full use of light energy. It applies photovoltaic effect to generate electricity as well as photo thermal effect to produce heat. The gravity heat pipe is installed in the back surface of the solar panel, so that heat from the solar panel can be guided into the house.
3. The system can obviously improve the efficiency of the solar photovoltaic on the market without changing the structure of solar panel.

### 4.2.2 The structure of the system

The solar air conditioning / heating system is shown as Fig. 16, and it consists of the solar panels, heating pump, gravity heat pipe, indoor and outdoor heat exchanger. The working principle of the system is that under normal working conditions of the solar cell, the heat of battery panel is taken away by the flow of the working fluid, water and water vapor, in the gravity heat pipe made of copper materials. In the wind tunnel, the heat is exchanged between pipe and fin by convection. Through the density difference between hot and cold air, the hot air is brought into indoor to heat the room. In summer, solar radiation are so abundant that electricity generated by the solar panels can drive heat pumps to accomplish endothermic cooling.



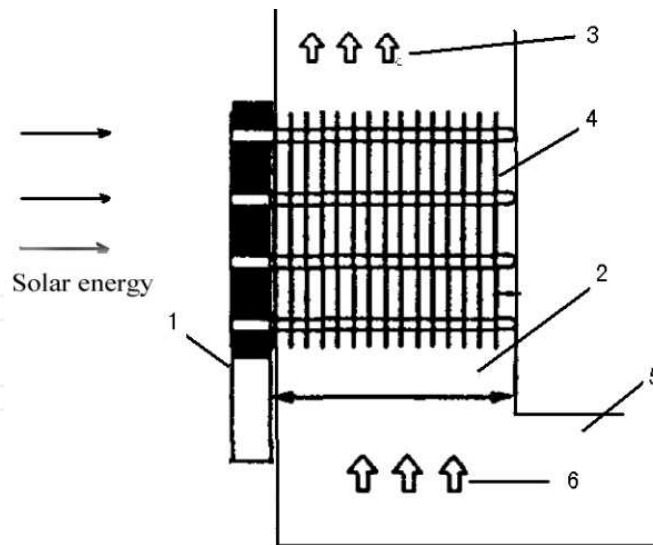
1. Solar panels 2. Outdoor air heat exchanger 3. Power supply 4. Compressor 5. A warm air outlet 6. Expansion valve 7. Air heat exchanger 8. Power supply 9. Heat pipe and fin 10. Cold wind inlet

Fig. 16. The structure of solar air conditioning / heating system

### 4.2.3 The system processing

#### a. The heat exchanger composed of heat pipe and fin

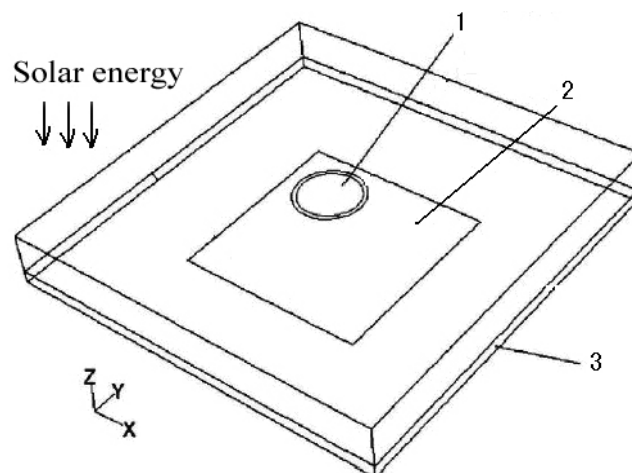
Heat pipe is a high efficient heat transfer element, which can transfer large amount of heat with a small area. The heat of the solar battery plate can be concentrated by the heat pipe through its one-way heat conduction. Gravity heat pipe without a capillary structure has the advantages of simple structure and convenient manufacturing process, and liquid returns naturally to the evaporator by gravity, so the working fluid flow is stable and reliable. At the same time, it's flexible for piping arrangements. Compared with the capillary structure of heat pipe, it is easier to design and its cost is much lower. So it can adapt to most situations, however the position of the condenser must be higher than the evaporation end. The schematic diagram of heat exchanger composed of heat pipes and fins is shown as Fig. 17.



1. Solar panel 2. Cooling section 3. Warm air 4. Fins 5. Hot air channel 6. The cold wind  
Fig. 17. Schematic diagram of heat exchanger composed of heat pipes and fins

#### b. The connection between solar panels and heat pipes

The gravity heat pipe cooling mode is adopted in the system and water is the working substance. For the heat pipe, the design of evaporation end is an important part, which directly affects its ability to deal with the heat produced in solar concentrator photovoltaic cells and the ability to control its temperature. A good design of the evaporation end should ensure evaporation end transfer enough heat to make the operating temperature of the solar concentrator photovoltaic cell as low as possible, not exceeding the critical temperature, enabling it to continue working properly. The evaporation end of the heat pipe contacts the concentrator solar cells, and its temperature field has an obvious effect on performance of the battery and efficiency of the heat pipe. In this chapter, the evaporation end is designed as a cuboid with the dimensions of length 100mm, width 100mm and height 30mm. The diagram of the heat pipe on solar evaporation end is shown as Fig. 18.



1. Gravity heat pipe 2 Layer of metal thermal conductivity 3 the back surface of solar panels  
Fig. 18. The connection diagram of solar panels and heat pipes

### c. Throttle switch

In summer, the air damper is put downward, which separates the vertical air channel from the horizontal air channel, letting the hot air directly emit into the atmosphere. While in the winter, the air damper is put upward, so the vertical and horizontal air channels are connected, letting the system heat the indoor room.

## 4.3 The theoretical analysis of experimental data on the solar energy air conditioning / heating system

### 4.3.1 Cases in the summer

The photoelectric conversion efficiency of solar panels on the market is 16%, and it drops about 0.5% with each 1°C rising of the temperature. In this chapter, TRM-PD artificial sun simulation emitter, whose light intensity ranges from 0 to 800 W/m<sup>2</sup>, is adopted, from which the solar panels receive the simulated illumination.

The parameters of the equipment are as follows:

- The heat-absorbing plate: 1 mm thickness of copper plate painted black to reduce the reflection to enhance absorption effect
- The transparent cover: ordinary glass with dimension of 505 × 490 × 4 mm
- The thermal insulation layer: glass silk, with around 5 cm of thickness
- The solar panels: its power is 20 W, working voltage 17.6 V, working current 1.14 A, open circuit voltage 21.6 V, short-circuit current 1.33 A, with dimension of 426 × 406 × 30 mm

The average values of the measured data of the solar panels are shown as Table 5.

$$P_{average} = \frac{\sum_{i=1}^n P_{Total\ i}}{n} = 17.18W \quad (9)$$

The light intensity output of solar energy simulator in the experimental system is 800W, and the effective area of the solar energy panels is 400 mm × 300 mm, so the input power of panels is:

$$P_{inlet} = 96W \quad (10)$$

Without a cooling device, the solar energy utilization  $\eta_1$  is:

$$\eta_1 = \frac{P_{average}}{P_{inlet}} \times 100\% = 11.8\% \quad (11)$$

Adding the cooling device, the solar energy utilization  $\eta_2$  is :

$$\eta_2 = \frac{P_{average}}{P_{inlet}} \times 100\% = 17.8\% \quad (12)$$

It can be inferred that after adding the cooling device, the solar energy utilization rate is increased  $\Delta\eta = \eta_2 - \eta_1 = 6\%$ . Under this condition, with solar panels area of  $8\text{m}^2$ , the electric power output is

$$P = 558.66\text{W} \quad (13)$$

| Flux (L/min) | Inlet Temperature (°C) | Outlet temperature (°C) | Surface temperature of battery board (°C) | Atmospheric temperature (°C) | Voltage(V) | Current(A) |
|--------------|------------------------|-------------------------|---|------------------------------|------------|------------|
| 2.647        | 28.809                 | 45.718                  | 57.262                                    | 29.581                       | 10.083     | 0.1246     |
| 3.103        | 29.155                 | 50.780                  | 59.591                                    | 30.258                       | 10.088     | 0.1170     |
| 7.895        | 27.808                 | 38.633                  | 61.242                                    | 29.770                       | 9.940      | 0.1216     |
| 15.000       | 28.012                 | 34.551                  | 62.582                                    | 30.506                       | 9.962      | 0.1201     |
| 27.692       | 28.088                 | 34.271                  | 63.084                                    | 30.169                       | 10.152     | 0.1176     |
| 36.000       | 28.049                 | 31.356                  | 62.128                                    | 30.409                       | 10.076     | 0.1167     |

Table 5. The average of the measured data during each flow period

#### 4.3.2 Cases in the winter

The winter condition is also designed according to performance parameters of the solar battery and the heat pipe installation model as mentioned above. It is assumed that the solar radiation intensity is  $400\text{W}/\text{m}^2$ , the average temperature of solar panels is  $55^\circ\text{C}$ , the average temperature of the heat pipe and fins  $t_f' = 40^\circ\text{C}$ , inlet temperature  $t_f'' = 10^\circ\text{C}$ , heat length is  $2.5\text{m}$ , and air flow velocity  $u_m = 2\text{m}/\text{s}$ .

Heat exchanging unit of this system is shown as Fig. 19.

Assuming air temperature at the outlet  $t_f'' = 25^\circ\text{C}$ , then the qualitative temperature  $t_f = (10 + 25)^\circ\text{C} / 2 = 17.5^\circ\text{C}$ , and the corresponding physical parameters of air are  $\lambda = 0.0276\text{W}/(\text{m}\cdot\text{K})$ ,  $\nu = 16.96 \times 10^{-6}\text{m}^2/\text{s}$ ,  $\text{Pr}_f = 0.699$ , and  $\eta_f = 19.1 \times 10^{-6}\text{Pa}\cdot\text{s}$ .

It can be inferred that

$$\text{Re}_f = \frac{ud}{\nu} = 11793 > 10^4 \quad (14)$$

The air flow in the turbulent field,

$$\text{Nu}_f = 0.023\text{Re}_f^{0.8}\text{Pr}_f^{0.4} = 30.752 \quad (15)$$

$$h_f = \text{Nu}_f \frac{\lambda}{d} = 8.7\text{W}/(\text{m}^2\cdot\text{K}) \quad (16)$$

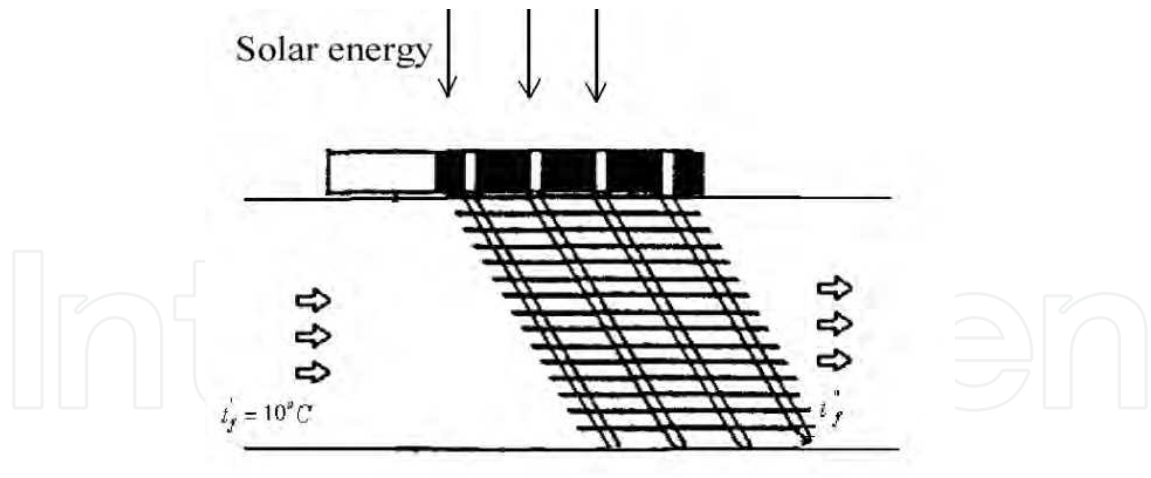


Fig. 19. Heat exchanging unit of this system

According to the assumed exit temperature, the logarithmic mean temperature difference of air flow along the total tube length is equal to

$$\Delta t_m = \frac{t_f'' - t_f'}{\ln[(t_f' - t_w) / (t_f'' - t_w)]} = 22.46^\circ C \tag{17}$$

According to the surface heat transfer coefficient, the quantity of convective heat transfer can be calculated as

$$\Phi_1 = h_f 4l \Delta t_m = 522W \tag{18}$$

According to the flow rate and the temperature rising from inlet to outlet, the total heat exchanging can be calculated as

$$\Phi_2 = q_m c_p (t_f'' - t_f') = 445.3W \tag{19}$$

The results of two total heat exchanging don't match each other because the assumed outlet temperature is not correct. Through the iterative computation to eliminate deviation, the result is:

$$h_f = 8.32W / (m^2 \cdot K), \quad t_f'' = 22.4^\circ C, \quad \Phi = 467W \tag{20}$$

Under winter heating condition, the reachable heat output of exchanger is 467 W.

### 5. Research on the solar drying system

In some countries, such as in China, sometime clothes are suspended outside the window to dry, which are uneven in length, affecting the scene of the city, and the water drop may either wet passers-by or commodities. At the same time, domestic appliances are getting more various to meet the modern living, making it possible to design a novel device to combine the existed domestic appliances to dry the clothes besides their existing functions.

In this chapter, a novel device is designed to connect with solar energy collector, and it can also be connected to domestic solar water heater to effectively use excess energy of the solar water heater. The device mainly consists of insulation shell, heat transfer system, ventilation system, drainage system, temperature humidity control system, ultraviolet radiation sterilization disinfection system and some auxiliary systems. Compared with the published patents, this device just needs a small area, and it can work under a complete indoor situation of natural environment. It is installed with ultraviolet disinfection lights and hollowed aromatherapy box, so it may sterilize clothes and fresh the air during drying clothes so as to achieve better results than clothes are dried outside the window. This device may be effectively applied to lots of occasions, such as families, hotels, schools and so on. It shows high practical value and economic and social benefits.

### **5.1 Backgrounds of the solar drying system**

The high price of the house and apartment is an outstanding issue in modern society, so that small living space becomes very popular in some regions. To save space, the clothes are suspended outside the window to dry. If a sudden rain happens, clothes will be wet and dirty again. In order to solve this problem to help people living more convenient, some devices using solar energy to dry clothes have been on the market, while they can only be used outdoor. The authors have designed a kind of solar drying system, which occupies a small area so that it may be installed in the house, and has the same drying effect as the clothes are put outside the window.

At present, there is no similar device on the market yet, and sometime warm air blower or electrical heater is used to dry clothes for emergencies, which consumes a lot of energy and seriously damages the clothes, so it is not a good choice for a long time.

Solar energy water heater are widely used in lots of region, so if we can link solar energy water heater with a drying oven, using its original power cycle system to make hot water circulate in the designed oven and the heat flow through the pipe to distribute inside the box, the clothes will be dried quickly with the convection of hot air. The device can accomplish this function in small indoor space. It can not only make full use of the solar energy water heater during idle time, but also can shorten the drying time, so it may increase the solar energy utilization efficiency and improve the quality of people's daily life.

### **5.2 Technical requirements on the solar drying system**

For the solar energy dryer, due to its small working area, long working hours, and strong dependence on the weather, the following specifications are required:

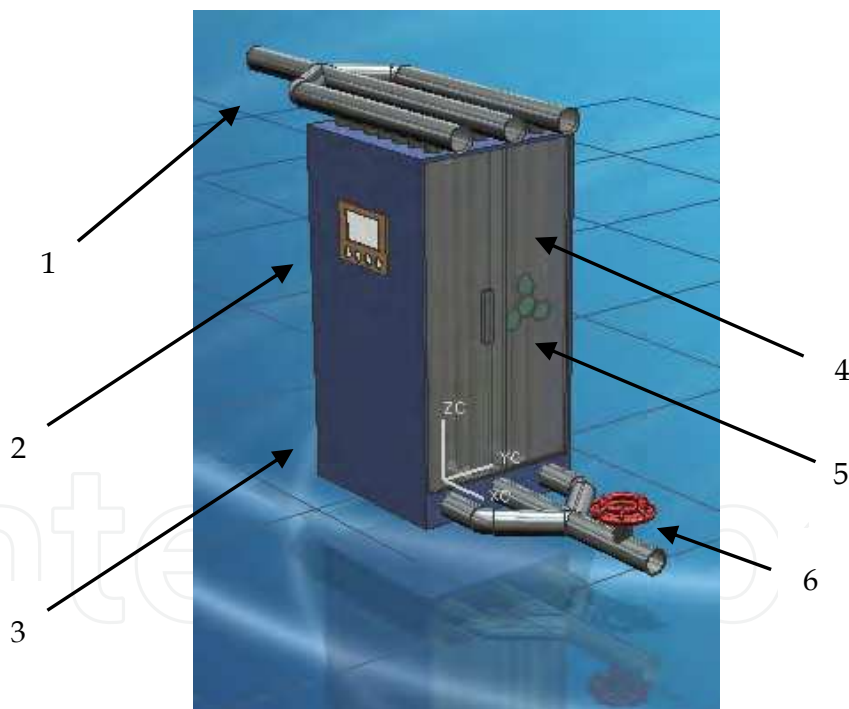
1. Materials with good heat conduction performance are used to manufacture the pipe in the oven, so that they can absorb the maximum quantity of heat from hot water to ensure a high constant temperature of the oven.
2. Ultraviolet disinfection lamp is installed in the oven to sterilize the clothes, which can make the dryer arrive at the unique advantage of drying out of the window as far as possible.
3. A small fan is installed in the oven. It not only accelerates the wet loss of moisture, making humid air quickly spread to the external to increase dryness of the internal air, but also strengthens the flow of hot air to improve drying efficiency.

4. A hollowed aromatherapy box is specially installed inside the oven, so that the clothes will have a light faint scent, making our body more comfort.
5. The probes of thermometer and humid meter are installed inside the oven, which can readily record the temperature and humidity. The flow valves at the bottom of the box may be adjusted to control the heat transfer according to the feedback of temperature and humidity together with the materials of the clothes.
6. Thermal insulation material is installed up and down and back and forth of the dryer to prevent heat loss. The left and right sides are made of movable glass, so it is easy to put the clothes into the oven, and adjust ventilation rate according to temperature and humidity.
7. The drying oven and solar energy collector share one set of power cycle system.

### 5.3 Design scheme of solar drying system

#### 5.3.1 The main body structure of solar drying system

The solar drying system not only needs to solve the city image problem due to clothes being hanged to dry outdoor, but also needs to simulate the situation of drying outdoor as far as possible. For example, the sterilization of outdoor sunlight and other characteristics need to be reflected in the design, making it come from the nature and be better than the natural



1. Heat transfer conduit
2. Thermo-humidometer
3. Heat preservation box shell
4. Movable glass door
5. Fan
6. The regulator

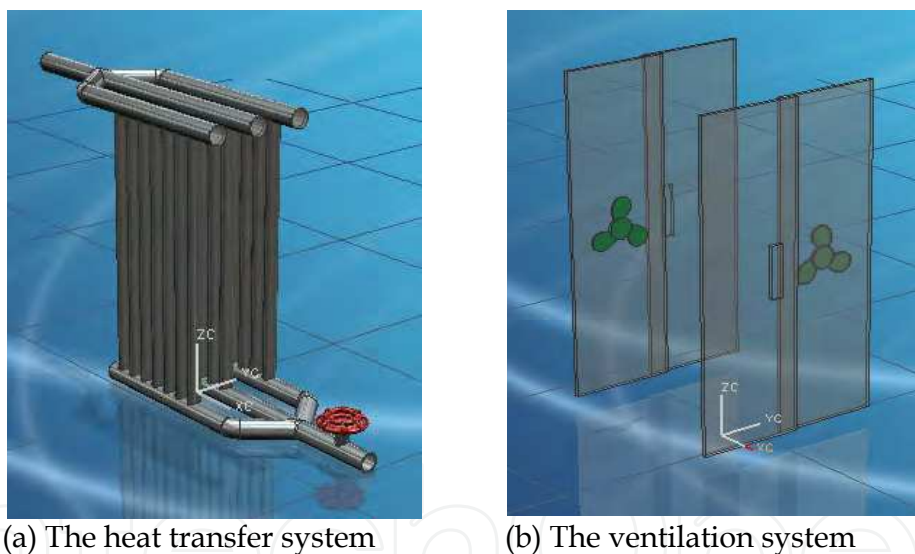
Fig. 20. Main body structure design of solar drying oven

The main body structure of the solar drying device is shown as Fig. 20. It demonstrates that the main body of the solar drying device includes ultraviolet disinfection system, ventilation system, temperature and humidity control system, drainage system, heat transfer system and additional system.

### 5.3.2 Heat transfer and ventilation system

Heat transfer system is the main system of the drying device. In order to increase the relative area of the heat transfer, three rows of pipe with staggered pattern are added within limited space conditions, dividing the oven into two parts so as to let clothes be hanged between the pipe rows. The heat transfer system is shown as Fig. 21(a). Hot water flows in the pipe and convection heat transfer happens between pipelines, heat transfer between pipeline walls is conduction, and heat is transferred to the clothes in the oven through thermal radiation and convection. Because the hot water in the unceasing cycle ensures the heat supply, and the pipe made of good thermal conductivity material has good heat transfer characteristics, the heat loss is strongly reduced to the minimum to increase the heat transfer efficiency.

The ventilation system is necessary in the drying device. It is confirmed through a large number of experiments that during clothes drying, because the air is too wet, movable glass of drying device are full of water mist so that drying effect is greatly reduced. To solve this problem, a small speed-adjustable fan is installed, which can not only appropriately speed up the wet loss of air according to the practical situation, but also accelerate the hot air convection. Ventilation system is shown as Fig. 21(b). In addition, both sides of movable glass walls can regulate ventilation rate according to the specific situation.



(a) The heat transfer system

(b) The ventilation system

Fig. 21. The diagram of the heat transfer and ventilation system

### 5.3.3 Temperature and humidity control system

In order to achieve better drying effect and reflect people-oriented design concept, a temperature and humidity control system is installed with the probes of the thermometer and humidity meter being inserted into the oven. The probes can sensitively detect the internal temperature and air humidity and digitally display on the external side of the box. The flow control valves at the bottom of the oven is adjusted by evaluating data on the meters, the material of the clothes and its drying difficulty level to change the hot water velocity, in turn, change the heat flux. Temperature and humidity control system is shown as Fig. 22.

### 5.3.4 Drainage system

The clothes are now usually washed by washing machine, and then most water is eliminated by a spin-drier, so that the water remaining in the clothes is relatively low, and the clothes would be much easier to dry. However, not all the clothes are washed with a washing machine, especially those small ones in the summer are usually washed by hand. Based on this consideration, the bottom of this drying machine is designed as four corners so that dripping water can deviate from the drain outside the oven by their own gravity. Drainage system is shown as Fig. 23.

### 5.3.5 Ultraviolet sterilization system

Except for the limited indoor space, the main reason people hang clothes out in the sun is to get the sterilization effect of the ultraviolet rays in sunlight to make clothes more clean and fresh. In order to simulate outdoor conditions completely, two ultraviolet disinfection tubes are installed on the top side inside the dryer so as to reach natural ultraviolet ray sterilization effect.

### 5.3.6 Auxiliary system

In order to let solar drying machine more considerate to provide more practical assistance to people's life, a hollow aromatherapy box is installed inside the oven, which makes the clothes more pure and fresh during drying. And the hollow box is removable, and people can replace box spices according to their favorite tastes.

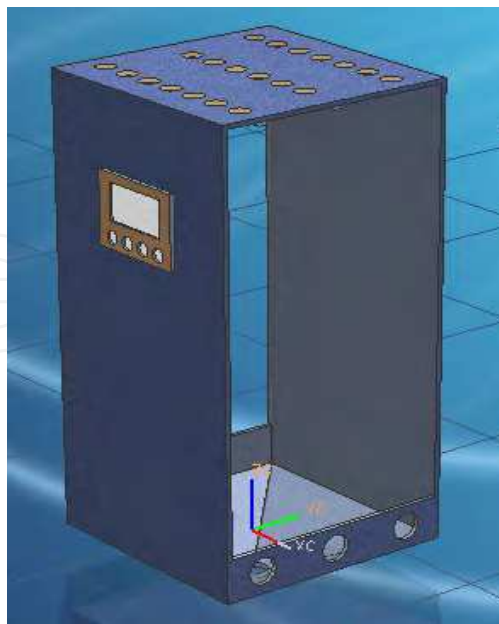


Fig. 22. Thermo-humido-control system

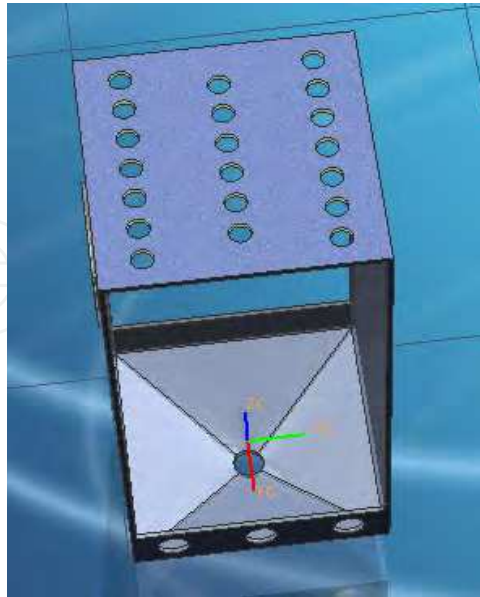


Fig. 23. Drainage system



Fig. 24. Solar drying machine system

#### 5.4 Device characteristics

The invented solar drying machine can illustriously combine with solar water heater, adjust the heat flux and ventilation rate, accommodate all kinds of clothes, and dry quickly. It has a good performance to work for a long time in good sunlight, and it has a high stability, reliability, and strong practicability. The whole system is shown as Fig. 24.

## 6. Summary

As one kind of inexhaustible, safe, energy saving, environmental protective new energy, solar energy is getting more and more attention in this world and it has a huge development potential. Through the research of solar flat-plate collector, staged solar photovoltaic and thermal collector, solar air-conditioning system and solar drying system, the authors explore a research and developing approach of solar energy.

## 7. References

- [1] Grasse W. Solar PACES Annual Report. DLR Germany, 1998.
- [2] Rabl A., Optical and thermal properties of compound parabolic concentrator, *Solar Energy*, 1976(18): 497-511.
- [3] Kostic LT, Pavlovic TM, Pavlovic ZT. Influence of reflectance from flat aluminum concentrators on energy efficiency of PV/Thermal collector, *Applied Energy*, 2010(87): 410-416.
- [4] Chiasson A.D., C. Yavuzturk, Assessment of the viability of hybrid geothermal heat pump systems with solar thermal collectors, *ASHRAE Transactions*, 2003, 109 (2): 487-500.
- [5] Ozgener O., Hepbasli A., A review on the energy and energy analysis of solar assisted heat pump systems, *Renewable and Sustainable energy reviews*, 2007(11): 482-496.
- [6] Dossier Géothermie, *Revue bimestrielle Systèmes solaires - L'observateur des énergies renouvelables*, 2002(148): 20-60.
- [7] Hellstrom B, Adsten M, Nostell P, Karlsson B, Wackelgard E., The impact of optical and thermal properties on the performance of flat plate solar collectors, *Renew Energy*, 2003(28): 331-344.
- [8] Tanaka H, Nakatake Y., Improvement of the tilted wick solar still by using a flat plate reflector. *Desalination* 2007(216): 139-146.
- [9] Tanaka H, Nakatake Y., Increase in distillate productivity by inclining the flat plate external reflector of a tilted-wick solar still in winter, *Solar Energy*, 2009(83): 785-789.
- [10] Tanaka H., Tilted wick solar still with external flat plate reflector: optimum inclination of still and reflector, *Desalination*, 2009(249): 411-415.
- [11] S.X. Yi, H.X. Sheng, F.F. Wang, Test of ventilation and lowering moisture on late indica rice of high moisture content in large warehouse, *Grain Storage*, 2005(35): 32-34.
- [12] Jain D., Modeling the performance of the reversed absorber with packed bed thermal storage natural convection solar crop dryer, *J Food Eng*, 2007(78): 637-647.
- [13] Alvarez A., Cabeza O., Muñiz MC., Varela LM., Experimental and numerical investigation of a flat-plate solar collector, *Energy*, 2010(35):3707-3716.
- [14] Henning H-M., editor. *Solar assisted air-conditioning in buildings—a handbook for planners*. ISBN3-211-00647-8, Wien: Springer, 2004.
- [15] Syed A., Maidment G., Missenden J., Tozer R., Optimal solar cooling systems. HPC 2004, the third international conference on heat powered cycles, Larnaca, 10-13 October, Cyprus, 2004.
- [16] Carrier product data, active and passive chilled beams, model 36CBPB14, Carrier Corporation, 2008.

- [17] Matsui H., Okada K., Kitamura T., Tanabe N., Thermal stability of dye-sensitized solar cells with current collecting grid, *Energy Mater Sol Cells*, 2009(93): 1110-1115.
- [18] H. Liu, L.L. Zhang, L.M. Ren, The in-store drying experiment of high moisture content by mechanical ventilation, *Journal of Henan University of Technology*, 2007 (28): 22-25.
- [19] K. Daou, R.Z. Wang, Z.Z. Xia, Desiccant cooling air conditioning: a review, *Renewable Sustain Energy Rev.*, 2006(10): 55-77.
- [20] Akhtar N., Mullick SC., Computation of glass-cover temperatures and top heat loss coefficient of flat-plate solar collectors with double glazing, *Energy*, 2007(32): 1067-1074.
- [21] Madhlopa A., Ngwalo G., Solar dryer with thermal storage and biomass-backup heater, *Solar Energy*, 2007(81): 449-462.

IntechOpen



## **Solar Power**

Edited by Prof. Radu Rugescu

ISBN 978-953-51-0014-0

Hard cover, 378 pages

**Publisher** InTech

**Published online** 15, February, 2012

**Published in print edition** February, 2012

A wide variety of detail regarding genuine and proprietary research from distinguished authors is presented, ranging from new means of evaluation of the local solar irradiance to the manufacturing technology of photovoltaic cells. Also included is the topic of biotechnology based on solar energy and electricity generation onboard space vehicles in an optimised manner with possible transfer to the Earth. The graphical material supports the presentation, transforming the reading into a pleasant and instructive labor for any interested specialist or student.

### **How to reference**

In order to correctly reference this scholarly work, feel free to copy and paste the following:

Jiang Wu and Jianxing Ren (2012). Research and Application of Solar Energy Photovoltaic-Thermal Technology, Solar Power, Prof. Radu Rugescu (Ed.), ISBN: 978-953-51-0014-0, InTech, Available from: <http://www.intechopen.com/books/solar-power/research-and-application-of-solar-energy-photovoltaic-thermal-technology>

**INTECH**  
open science | open minds

### **InTech Europe**

University Campus STeP Ri  
Slavka Krautzeka 83/A  
51000 Rijeka, Croatia  
Phone: +385 (51) 770 447  
Fax: +385 (51) 686 166  
[www.intechopen.com](http://www.intechopen.com)

### **InTech China**

Unit 405, Office Block, Hotel Equatorial Shanghai  
No.65, Yan An Road (West), Shanghai, 200040, China  
中国上海市延安西路65号上海国际贵都大饭店办公楼405单元  
Phone: +86-21-62489820  
Fax: +86-21-62489821

© 2012 The Author(s). Licensee IntechOpen. This is an open access article distributed under the terms of the [Creative Commons Attribution 3.0 License](#), which permits unrestricted use, distribution, and reproduction in any medium, provided the original work is properly cited.

IntechOpen

IntechOpen